Acta Polytechnica **62**(6):595–606, 2022
https://doi.org/10.14311/AP.2022.62.0595

PARAMETRIC STUDY OF THE ENERGY POTENTIAL OF A BUILDING'S ENVELOPE WITH INTEGRATED ENERGY-ACTIVE ELEMENTS

Daniel Kalús[a], Daniela Koudelková[a], Veronika Mučková[a], Martin Sokol[a], Mária Kurčová[a], Patrik Šťastný[b,*]

[a] *Slovak University of Technology in Bratislava, Faculty of Civil Engineering, Department of Building Services, Radlinského 11, 810 05 Bratislava, Slovakia*

[b] *Slovak University of Technology in Bratislava, Faculty of Civil Engineering, Department of Building Technology, Radlinského 11, 810 05 Bratislava, Slovakia*

[*] corresponding author: patrik.stastny@stuba.sk

Abstract.

Building structures with integrated energy-active elements (BSIEAE) present a progressive alternative for building construction with multifunctional energy functions. The aim was to determine the energy potential of a building envelope with integrated energy-active elements in the function of direct-heating, semi-accumulation and accumulation of large-area radiant heating. The research methodology consists in an analysis of building structures with energy-active elements, creation of mathematical-physical models based on the simplified definition of heat and mass transfer in radiant large-area heating, and a parametric study of the energy potential of individual variants of technical solutions. The results indicate that the increase in heat loss due to the location of the tubes in the structure closer to the exterior is negligible for Variant II, semi-accumulation heating, and Variant III, accumulation heating, as compared to Variant I, direct heating, it is below 1 % of the total delivered heat flux. The direct heat flux to the heated room is 89.17 %, 73.36 %, and 58.46 % of the total heat flux for Variant I, Variant II and Variant III, respectively. For Variant II and Variant III, the heat storage accounts for 14.84 %, and 29.86 % of the total heat flux, respectively. Variants II and III appear to be promising in terms of heat/cool accumulation with an assumption of lower energy demand (at least 10 %) than for low inertia walls. We plan to extend these simplified parametric studies with dynamic computer simulations to optimise the design and composition of the panels with integrated energy-active elements.

Keywords: Building Structures with Integrated Energy-Active Elements (BSIEAE), Active Thermal Protection (ATP), Thermal Barrier (TB), Large-Scale Radiant Heating/Cooling (LSRHC), Heat/Cool Accumulation (HCA), Absorption of Solar and Ambient Energy, Thermally Activated Building Structure (TABS).

1. Introduction

Mass production of prefabricated panels and standardised building modules with integrated energy-active elements represents a variant of building construction with advantages in the form of fast assembly of building objects with combined building-energy systems without significant technological downtime, higher economic efficiency, high potential for the use of renewable energy sources (RES) and waste heat. These facts inspire and motivate us to research different variants of technical solutions of self-supporting panels with an internal energy source, active thermal protection (ATP), which we have described in the utility model SK5729 Y1 [1], thermal insulation panels for systems with active heat transfer control in utility model SK5725 Y1 [2], and in the European patent EP 2 572 057 B1 "Heat insulating panel with active regulation of heat transition" [3].

Active thermal protection (ATP) is a dynamic process characteristic of building structures with integrated energy-active elements characterised by one or more functions in different energy systems' operation modes. The energy functions of ATP are a thermal barrier, large-scale radiant low-temperature heating/high-temperature cooling, heat/cold storage, solar and ambient energy capture, heat/cold recovery, heat recovery, etc. This study aims to determine the energy potential of a building envelope with integrated energy-active elements in the function of direct-fired, semi-accumulation (TABS system), and accumulation of large-area radiant heating.

2. Current situation

Various designs of prefabricated panels and standardised building modules with integrated energy-active elements are known. According to the energy function, building structures with active thermal protection (ATP) are divided into:

- building structures with large-scale radiant low-temperature heating or high-temperature cooling (BSHC) function, Figure 1,
- building structures with thermally activated building structure (TABS) function, Figure 2,

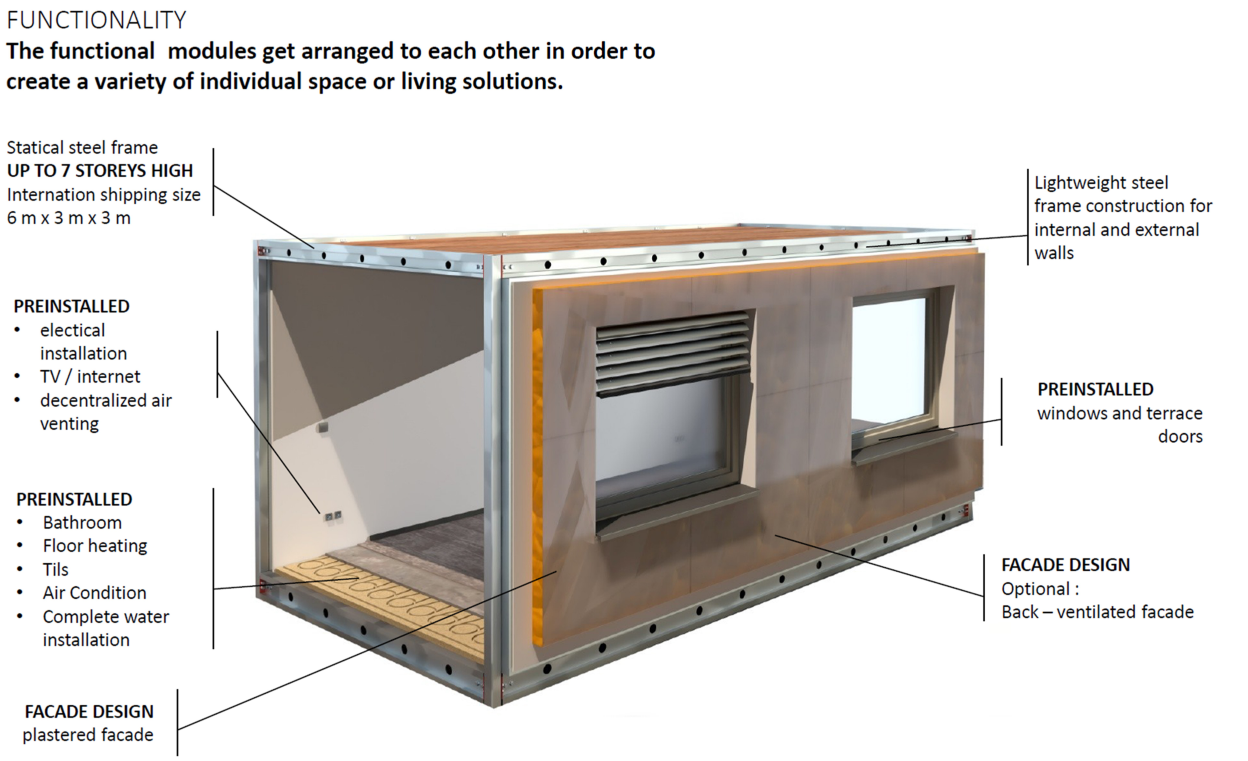

Figure 1. Standardised SUNOMAXCUBE building module with integrated energy-active elements in the building structures [4].

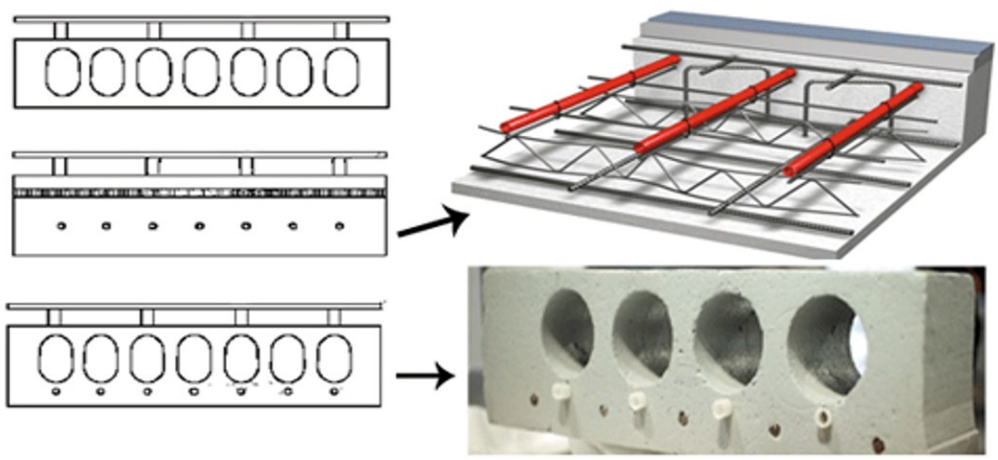

Figure 2. Division of TABS according to the position of the heat transfer medium: In the upper part: the heat transfer medium is air distributed through the cavities in the ceiling panel, in the middle: the heat transfer medium is a liquid in a pipe – monolithic ceiling, in the lower part: the heat transfer medium is a liquid in a pipe – prefabricated ceiling panel [5].

- building structures with thermal barrier function (TB), Figure 3,
- building structures with an absorber (BSA) built into the building structure on the outside of the building envelope to capture solar or ambient energy in synergy with heat pumps, Figure 4,
- building structures with combined energy functions (BSCE), Figure 5.

Figure 1 shows a standardised SUNOMAXCUBE building module with integrated energy-active elements in the building structures [4]. One of the pre-installed energy systems is a large-area low-temperature radiant floor heating [6].

Thermally activated building structures (TABS) can also implement large-scale, low-temperature heating and high-temperature cooling. The term 'thermally activated parts' is used for structures in which the flow of a heat transfer fluid heats or cools the entire structure, and consequently the surrounding spaces. They are also called hybrid systems since building structures have started to be used as heat exchange surfaces. These systems operate at a small temperature difference between the temperature of the heat transfer fluid and the surrounding space, allowing them to use low-temperature energy sources. TABS are made up of structures characterised by high density, and weight (walls, ceilings, columns...) and equipped with cavities for air circulation, pipes for water circulation, or pipes embedded in the monolithic ceilings of multi-story buildings, Figure 2.

Figure 3. Left and centre – ISOMAX thermal barrier (TB) perimeter panel made of lost-foam expanded polystyrene formwork, on the right – panels comprehensively manufactured in the panel factory [7].

ISOMAX perimeter panels with an integrated thermal barrier (TB) consist of a lost-foam expanded polystyrene formwork containing a steel reinforcing mesh with piping, Figure 3. Usually, their internal space is filled with a cast-in-place concrete mix only after they have been placed on site. In the next stage, the concrete must cure and reach the required strength (approx. 28 days). This construction technique is called 'wet construction'. This is only applied in new buildings. Alternatively, the production of these panels can be carried out comprehensively in a prefabrication plant [7].

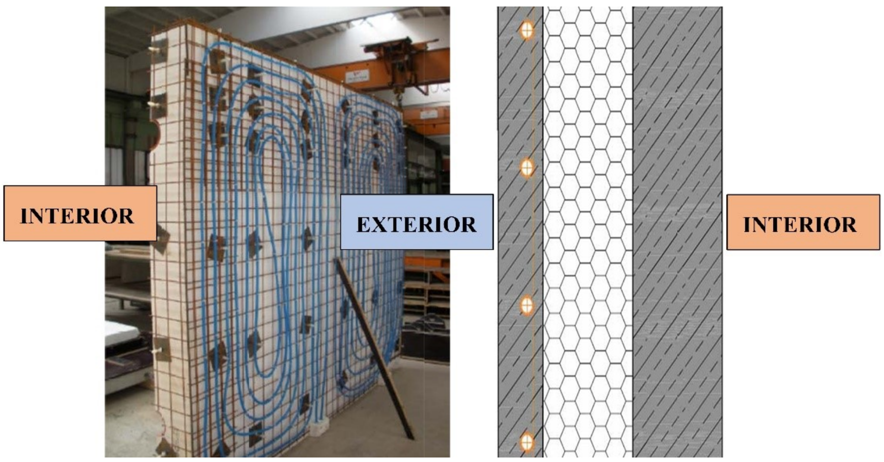

Figure 4. Single-pipe combined energy wall system with massive absorber [8].

One of the variants of building structures with absorber function embedded in the building structure on the exterior side of the building envelope used to capture solar or ambient energy in synergy with heat pumps is

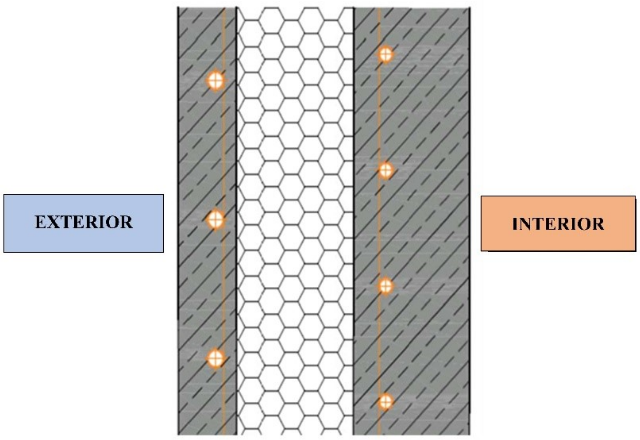

Figure 5. Double-pipe combined energy wall system with massive absorber [8].

shown in Figure 4. The composition of the wall structure is precisely defined. The first design solution used in practice is a wall with a reinforced concrete massive absorber (MA) on the outside, in which a plastic pipe is embedded [8]. The inner reinforced concrete core is separated from the massive absorber by a polyurethane foam layer separating the two reinforced concrete slabs. It is a polyurethane core that is sheathed on both sides with reinforced concrete. The single-walled combined energy wall system with a solid absorber is primarily used to capture energy from the exterior for further use with a heat pump. In theory, this system should also recover heat from the interior (without the use of a heat pump).

The two-tube combined energy wall system with a massive RIEDER absorber [8], Figure 5, is an improved version of the single-tube system, shown in Figure 4, by adding the energy functions of low-temperature heating and high-temperature cooling. The composition of the wall structure is well defined. The first design solution used in practice is a wall with a reinforced concrete massive absorber (MA) on the outside, in which a plastic pipe is embedded. The inner reinforced concrete core is separated from the MA by a layer of polyurethane foam which separates the two reinforced concrete slabs. It is a polyurethane core that is sheathed on both sides with reinforced concrete. In the inner reinforced concrete core, a plastic pipe is encased, which is used for heating and cooling. This system is also still in the experimental verification stage. It is envisaged that the massive absorber (MA) should capture heat from the exterior and serve as the primary circuit for the heat pump. The theoretical assumption is that the system should not only collect heat from the exterior but also recuperate the heat that spreads from the interior without the aid of the heat pump. The system will only be suitable for practical use if it absorbs more energy than the electrical energy required to drive the heat pump and circulators. The internal piping is used for the interior's low-temperature heating and high-temperature cooling.

Many researchers from all over the world have been involved in the analysis of building structures with integrated energy-active elements. We provide references to some of the main scientific studies in this area of research [9–25].

3. Methodology

The aim of this paper is a parametric study of the energy potential of precast reinforced concrete building envelope panels with integrated energy active elements in three energy functions, viz:

- direct heating; large-scale radiant low-temperature heating, VARIANT I,
- semi-accumulative (TABS system), VARIANT II,
- accumulation; large area radiant low-temperature heating, VARIANT III.

Based on the analysis of building structures with energy-active elements, Section 2, we have developed mathematical-physical models for selected variants of technical solutions of the panels based on a simplified definition of heat and mass transfer in radiant large-area heating, Figure 6–8. The parametric study of the energy potential of the different variants of the technical solutions is based on a simplified calculation according to [26–28]. In building structures with ATP, heat transfer is combined by convection and radiation. The heat exchange occurs on the inner and outer surfaces of the building structure. On the inside of the building structure, the following occurs:

- airflow, as the air is warmer in the higher positions and colder in the lower positions,
- radiation because of the heat exchange of a given structure with all other room structures.

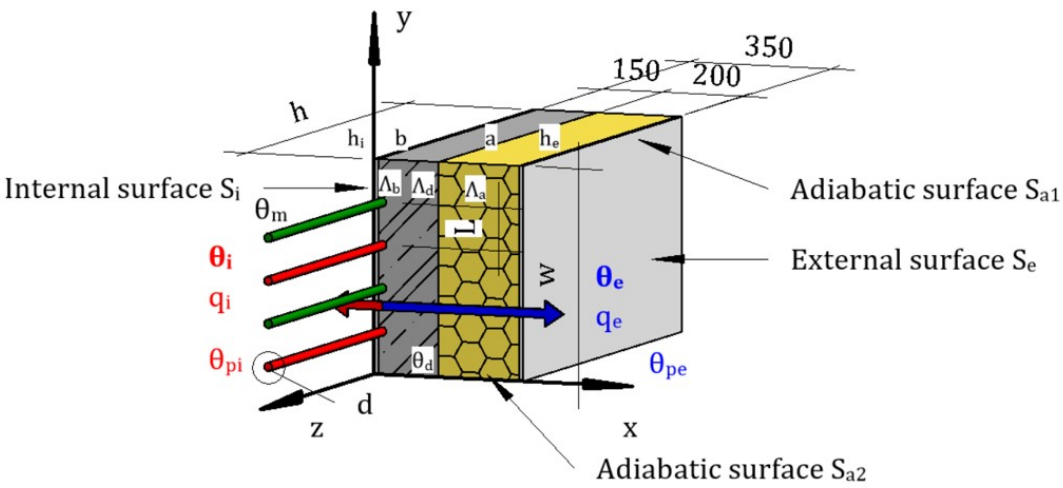

Figure 6. VARIANT I: Mathematical-physical model of a wall with integrated energy-active elements in the function of direct heating and cooling.
q_i – heat flow towards the interior [W m^{-2}], q_e – heat flow towards the exterior [W m^{-2}], θ_i – inside air temperature [°C], θ_e – outside air temperature [°C], θ_{pi} – interior surface temperature [°C], θ_{pe} – exterior surface temperature [°C], L – an axial distance of pipes [m], d – pipe diameter [m], Λ_a – thermal permeability of the layer in front of the pipes towards the interior [W (m^2 K)$^{-1}$], Λ_b – thermal permeability of the layer behind the pipes towards the exterior [W (m^2 K)$^{-1}$], Λ_d – thermal conductivity of the pipe material [W (m^2 K)$^{-1}$], θ_d – the average temperature of the structure in the axis of the pipes [°C], θ_m – average heating water temperature [°C], h_i – heat transfer coefficient towards the interior, h_e – heat transfer coefficient towards the exterior, a – thickness of the layer in front of the pipes [m], b – thickness of the layer behind the pipes [m].

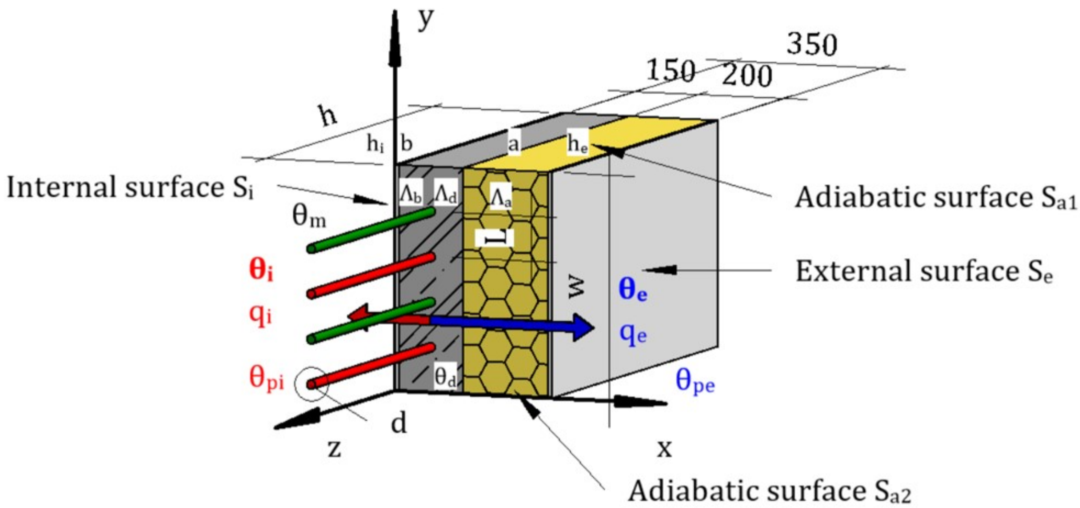

Figure 7. VARIANT II: Mathematical-physical model of a wall with an internal energy source located in the centre of the load-bearing part of a reinforced concrete panel, semi-accumulation heating and cooling, TABS system.
q_i – heat flow towards the interior [W m^{-2}], q_e – heat flow towards the exterior [W m^{-2}], θ_i – inside air temperature [°C], θ_e – outside air temperature [°C], θ_{pi} – interior surface temperature [°C], θ_{pe} – exterior surface temperature [°C], L – an axial distance of pipes [m], d – pipe diameter [m], Λ_a – thermal permeability of the layer in front of the pipes towards the interior [W (m^2 K)$^{-1}$], Λ_b – thermal permeability of the layer behind the pipes towards the exterior [W (m^2 K)$^{-1}$], Λ_d – thermal conductivity of the pipe material [W (m^2 K)$^{-1}$], θ_d – the average temperature of the structure in the axis of the pipes [°C], θ_m – average heating water temperature [°C], h_i – heat transfer coefficient towards the interior, h_e – heat transfer coefficient towards the exterior, a – thickness of the layer in front of the pipes [m], b – thickness of the layer behind the pipes [m].

On the outside of the building structure, there is:

- airflow mostly along with the structure due to wind,
- diffuse sky radiation acting on the building's surface, and the heat exchange between surrounding buildings and terrain [29].

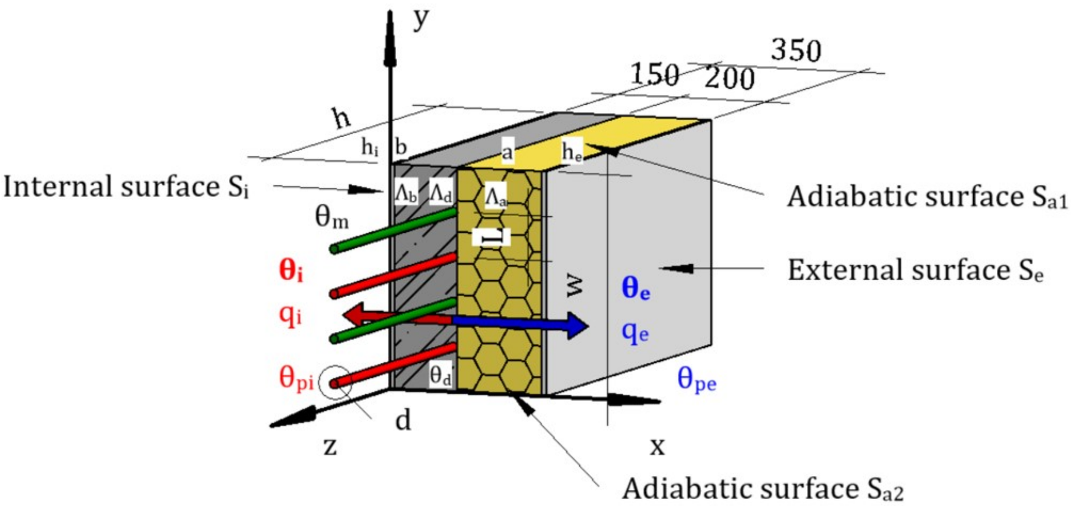

FIGURE 8. VARIANT III: Mathematical-physical model of a wall with integrated energy-active elements located at the interface between the load-bearing part and the thermal insulation part of the reinforced concrete panel, accumulation heating, and cooling system.
q_i – heat flow towards the interior [W m^{-2}], q_e – heat flow towards the exterior [W m^{-2}], θ_i – inside air temperature [°C], θ_e – outside air temperature [°C], θ_{pi} – interior surface temperature [°C], θ_{pe} – exterior surface temperature [°C], L – an axial distance of pipes [m], d – pipe diameter [m], Λ_a – thermal permeability of the layer in front of the pipes towards the interior [W (m^2 K)$^{-1}$], Λ_b – thermal permeability of the layer behind the pipes towards the exterior [W (m^2 K)$^{-1}$], Λ_d – thermal conductivity of the pipe material [W (m^2 K)$^{-1}$], θ_d – the average temperature of the structure in the axis of the pipes [°C], θ_m – average heating water temperature [°C], h_i – heat transfer coefficient towards the interior, h_e – heat transfer coefficient towards the exterior, a – thickness of the layer in front of the pipes [m], b – thickness of the layer behind the pipes [m].

To calculate the heat flux q [W m^{-2}] from ATP, we followed the procedure of [26–28]. The average temperature of the structure in the axis of the pipes:

$$\theta_d - \theta_i = (\theta_m - \theta_i) \cdot \frac{\tanh\left(m\frac{L}{2}\right)}{m\frac{L}{2}}, \tag{1}$$

where:

- θ_d the average temperature of the structure in the axis of the pipes [°C],
- θ_i internal design temperature [°C],
- θ_m average heating water temperature [°C],
- L axial distance of pipes [m],
- m coefficient characterising the heating plate in terms of heat dissipation [m^{-1}] [26–28].

Coefficient characterising the heating plate in terms of heat dissipation:

$$m = \sqrt{\frac{2 \cdot (\Lambda_a + \Lambda_b)}{\pi^2 \lambda_d d}}, \tag{2}$$

where:

- m coefficient characterising the heating plate in terms of heat dissipation [m^{-1}],
- Λ_a thermal permeability of the layer in front of the pipes towards the interior [W (m^2 K)$^{-1}$],
- Λ_b thermal permeability of the layer behind the pipes towards the exterior [W (m^2 K)$^{-1}$],
- λ_d thermal conductivity of the material into which the tubes are inserted [W (m K)$^{-1}$],
- d pipe diameter [m] [26–28].

Thermal permeability of the layer in front of the pipes towards the interior:

$$\Lambda_a = \sqrt{\frac{1}{\sum \frac{a}{\lambda_a} + \frac{1}{h_i}}}. \tag{3}$$

Thermal permeability of the layer behind the pipes towards the exterior:

$$\Lambda_a = \sqrt{\frac{1}{\sum \frac{b}{\lambda_b} + \frac{1}{h_e}}}, \tag{4}$$

where:

- Λ_a thermal permeability of the layer in front of the pipes towards the interior [W (m^2 K)$^{-1}$],
- Λ_b thermal permeability of the layer behind the pipes towards the exterior [W (m^2 K)$^{-1}$],
- a thickness of the layer in front of the pipes [m],
- b thickness of the layer behind the pipes [m],
- λ_a, λ_b thermal conductivity of the material of the respective layer [W (m.K)$^{-1}$],
- h_i heat transfer coefficient towards the interior [W (m^2 K)$^{-1}$],
- h_e heat transfer coefficient towards the exterior [W (m^2 K)$^{-1}$] [26–28].

The average surface temperature of the structure θ_p [°C]:

$$\theta_{pi} - \theta_i = \frac{\Lambda_a}{h_i} \cdot (\theta_d - \theta_i) = \frac{\lambda_a}{h_i} \cdot (\theta_m - \theta_i) \cdot \frac{\tanh\left(m\frac{L}{2}\right)}{m\frac{L}{2}}, \tag{5}$$

where:

- θ_{pi} the average surface temperature of the structure [°C],
- θ_d the average temperature of the structure in the axis of the pipes [°C],
- θ_i internal design temperature [°C],
- θ_m average heating water temperature [°C],
- Λ_a thermal permeability of the layer in front of the pipes towards the interior [W (m^2 K)$^{-1}$],
- Λ_b thermal permeability of the layer behind the pipes towards the exterior [W (m^2 K)$^{-1}$],
- h_i heat transfer coefficient towards the interior [W (m^2 K)$^{-1}$],
- L axial distance of pipes [m],
- m coefficient characterising the heating plate in terms of heat dissipation [m^{-1}] [26–28].

Specific heat output (flow) from the structure towards the interior:

$$q_i = \Lambda_a \cdot (\theta_d - \theta_i) = \alpha_p \cdot (\theta_p - \theta_i)\,, \tag{6}$$

and specific heat output (flow) from the structure towards the exterior:

$$q_e = \Lambda_b \cdot (\theta_d - \theta_i) = \Lambda_b \cdot \frac{h_i}{\Lambda_a} \cdot (\theta_{pi} - \theta_i) + \Lambda_b \cdot (\theta_i - \theta_e) \tag{7}$$

where:

- q_i heat flux from the structure towards the interior [W m^{-2}],
- q_e heat flux from the structure towards the exterior [W m^{-2}],
- θ_{pi} the average surface temperature of the structure [°C],
- θ_d the average temperature of the structure in the axis of the pipes [°C],
- θ_i calculated internal room temperature [°C],
- θ_e calculated external temperature [°C],
- Λ_a thermal permeability of the layer in front of the pipes towards the interior [W (m^2 K)$^{-1}$],
- Λ_b thermal permeability of the layer behind the pipes towards the exterior [W (m^2 K)$^{-1}$],
- h_i heat transfer coefficient towards the interior [W (m^2 K)$^{-1}$] [26–28].

4. Results and discussion

Based on the analysis of building structures with energy-active elements, Section 2, the developed mathematical-physical models, and the simplified calculation procedure according to [26–28], Section 3, we have developed an application calculator in Excel. We then calculated the following values for panel variants I, II, and III:

- θ_d average design temperature in the pipe axis [°C],
- θ_{pi} average surface temperature of the structure in the interior [°C],

- q_i heat flux from the structure towards the interior $[\mathrm{W\,m^{-2}}]$,
- q_e heat flux from the structure towards the exterior $[\mathrm{W\,m^{-2}}]$.

The calculation was conducted for a heating season. Boundary conditions include the following: the thickness of the reinforced concrete bearing part of the panel $b_{\text{panel}} = 150\,\mathrm{mm}$; thickness of the thermal insulation $b_{TI} = 200\,\mathrm{mm}$; outer dimension of the ATP pipe $d = 15\,\mathrm{mm}$; distance between pipes $L = 0.150\,\mathrm{m}$; heat transfer coefficient hp towards the interior $hp = 10\,\mathrm{W\,(m^2\,K)^{-1}}$ (according to EN 15377-1 [30] and STN 73 0540-2+Z1+Z2 [31]). According to [26–28], the average design temperature along the pipe's axis and the average surface temperature were calculated using simplified calculation relations that took into account the identical wall mass temperature in front of and behind the pipe. Figure 9 and Table 1 show the outcomes of the calculations for the heating period. The temperatures that were taken into account were the average working medium temperature in the ATP pipe $\theta_m = 30\,°\mathrm{C}$, the outside air temperature $\theta_e = -11\,°\mathrm{C}$, and the internal air temperature $\theta_i = 20\,°\mathrm{C}$.

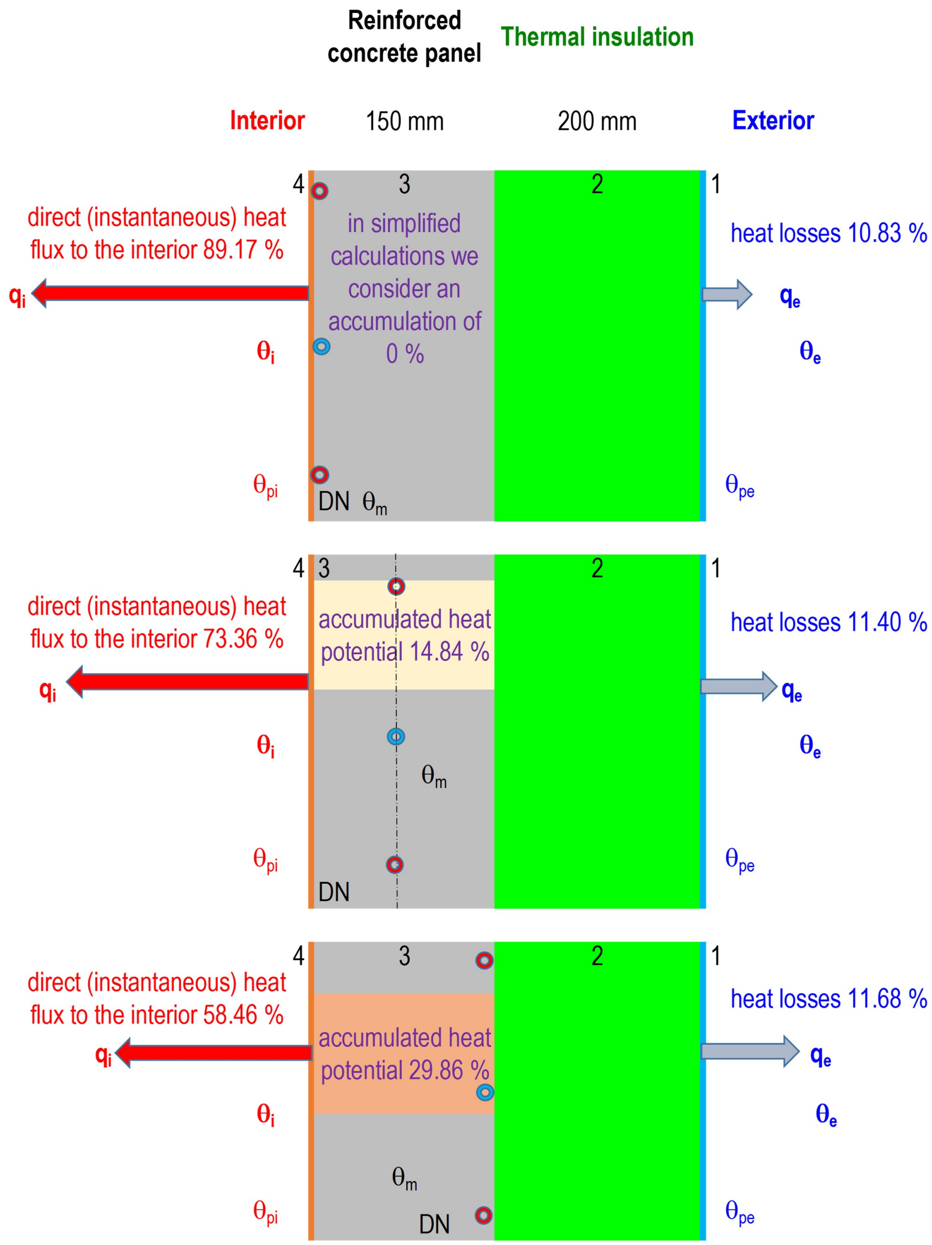

FIGURE 9. Heat flux analysis of the investigated variants of mathematical-physical models of perimeter reinforced concrete panels.
q_i – heat flow towards the interior $[\mathrm{W\,m^{-2}}]$, q_e – heat flow towards the exterior $[\mathrm{W\,m^{-2}}]$, θ_i – inside air temperature [°C], θ_e – outside air temperature [°C], θ_{pi} – interior surface temperature [°C], θ_{pe} – exterior surface temperature [°C].

Marginal conditions			Thermal transmittance behind/below the pipes towards the exterior Λ_a (W (m^2 K)$^{-1}$)	Thermal transmittance behind/below the pipes towards the exterior Λ_b (W (m^2 K)$^{-1}$)	Surface temperature temperature θ_p (°C)	Direct (instantaneous) heat flux to interior q_i (W m^{-2})	Direct (instantaneous) heat flux to exterior q_e (W m^{-2})	**Total direct (instantaneous) heat flux q_{direct} (W m^{-2})**	Accumulated heat flux in the building structure $q_{\mathrm{accumulation}}$ (W m^{-2})	**Total delivered heat flux q_{total} (W m^{-2})**	ratio of direct (instantaneous) heat flux to the exterior to the total direct (instantaneous) heat flux (%)	ratio of direct (instantaneous) heat flux to the exterior (instantaneous) heat flux to the exterior to the total delivered heat flux (%)	Comparison of direct (instantaneous) heat flux to the interior with conventional large area radiant heating (%)	Increase in losses of direct (instantaneous) heat flux to the exterior to losses to the exterior of conventional large area radiant heating (%)	Increase in losses of direct (instantaneous) heat flux to the exterior to the total delivered heat flux (%)
Interior temperature θ_i [°C] Exterior temperature θ_e [°C] Mean temperature of the heat transfer medium θ_m [°C]	20 -11 **30**	**Classic large-area radiant heating**	7.984	0.176	25.4855	54.854	6.663	**61.517**	0.000	**61.517**	10.83 %	10.83 %	100.00 %	0.00 %	0.00 %
Heat transfer coefficient before/above pipes to interior h_{pi} [W (m^2 K)$^{-1}$] Heat transfer coefficient behind the pipes to the exterior h_{pe} [W (m^2 K)$^{-1}$] Thermal conductivity coefficient TI λ [W/(m K)]	10 7 0.037	**Thermally Activated Building Systems (TABS)**	6.152	0.183	24.538	45.378	7.012	**52.390**	9.127	**61.517**	13.38 %	11.40 %	85.16 %	4.97 %	0.57 %
Pipe spacing L [mm] Pipe diameter [mm] Thermal insulation thickness (TI) [mm]	150 15 **200**	**Active thermal protection (ATP)**	4.542	0.185	23.596	35.963	7.186	**43.149**	18.368	**61.517**	16.65 %	11.68 %	70.14 %	7.28 %	0.85 %

Table 1. Partial results of the parametric study from the comparison of 3 variants of mathematical-physical models of panel design solutions.

In the parametric study of the stationary state based on mathematical-physical models and the analysis of the energy potential of the subject variants of panels with integrated energy-active elements, we considered heat and mass transfer with theoretical simplifications. For the panel with direct-fired large-area radiant heating, Variant I, we do not consider the accumulation of the delivered heat flux in the mass of the building structure. Table 1 shows the partial results from the parametric study, where all 3 variants of the mathematical-physical models of the panel design solutions are compared.

For thermal insulation in the thickness range of 50–100 mm, the heat flux to the interior q_i [W m^{-2}] increases while the heat loss q_e [W m^{-2}] decreases rapidly. For thicknesses above 100 mm, the effect of adding more insulation becomes relatively small. This is true regardless of the thickness of the concrete core, which has almost no effect on the heat flux. Conversely, the effect of pipe spacing on the heating performance is evident; despite the small effect on the heat flux to the interior, increasing the thickness of the concrete, and hence the inertia of the wall, can reduce the energy demand for heating [32]. For a system with a pipe embedded in a solid concrete core, the storage capacity, which is defined as a time constant, can range from roughly 2.5 to over 8 hours [33]. N. Aste, A. Angelotti, and M. Buzzetti, for instance, claim that in Milan, Italy, high-inertia walls can have an energy demand that is up to 10 % lower than low-inertia walls. S.A. Al-Sanea, M.F. Zedan, and S.N. Al-Hussain computed a reduction in energy demand for increasing wall thickness and heating energy savings of up to 35 % owing to thermal mass optimisation for the climate of Riyadh, Saudi Arabia [34]. In other research [35–37], the significance of concrete thickness for the thermal dynamics of buildings is highlighted. This importance must be taken into account when designing a new structure, a restoration, or a control system.

Based on the analysis of the energy potential of the various technical solutions for the envelope panels with integrated energy-active elements, it can be said that the increase in heat losses caused by the tubes' placement in the structure being closer to the exterior for Variant II, semi-accumulation heating (TABS system), and Variant III, accumulation heating, in comparison to Variant I, direct heating, is negligible, below 1 % of the total delivered heat flux, Table 1 and Figure 9.

Of the total supplied heat flux shown in Table 1 and Figure 9, the direct heat flux to the heated room is 89.17 % for direct heating, 73.36 % for semi-accumulation heating (TABS system), and 58.46 % for accumulation heating for Variant III.

VARIANT I ignores heat accumulation in favour of the panel's simplicity. According to Table 1 and Figure 9, Variant II represents 14.84 % and Variant III up to 29.86 % of the total supplied heat flux for the panel design (TABS system).

5. Conclusions

Variants II and III appear promising in heat/cool accumulation with an assumption of lower energy demand (at least 10 %) than for low inertia walls. We plan to extend these simplified parametric studies with dynamic computer simulations to optimise the design and composition of panels with integrated energy-active elements.

Research in building structures with integrated energy-active elements brings many inspirations, innovations, and completely new sustainable technical solutions that point to a high potential for energy savings, increased economic efficiency, and environmental friendliness. The predetermination of these building structures for the application of renewable energy sources and waste heat represents an energy-secure and self-sufficient technical solution as a fully-fledged alternative to energy systems dependent on fossil fuels.

Acknowledgements

This research was supported by the Ministry of education, Science, Research and Sport of the Slovak republic grant VEGA 1/0304/21. This research was supported by the Ministry of education, Science, Research and Sport of the Slovak republic grant KEGA 005STU-4/2021.

List of symbols

ATP Active Thermal Protection

BSA Building structures with an absorber

BSCE Building structures with combined energy functions

BSIEAE Building structures with integrated energy-active elements

BSHC Building structures with large-scale radiant low-temperature heating or high-temperature cooling

EP European patent

HCA Heat/cool accumulation

LSRHC Large-scale radiant heating/cooling

MA Massive absorber

RES Renewable Energy Sources

TABS Thermally Activated Building Structure

TB Thermal Barrier

TI Thermal insulation

a Thickness of the layer in front of the pipes [m]

b Thickness of the layer behind the pipes [m]

d Pipe diameter [m]

h_e Heat transfer coefficient towards the exterior $[\mathrm{W\,(m^2\,K)^{-1}}]$

h_i Heat transfer coefficient towards the interior $[\mathrm{W\,(m^2\,K)^{-1}}]$

L Axial distance of pipes [m]

m Coefficient characterising the heating plate in terms of heat dissipation $[\mathrm{m^{-1}}]$

q The heat flux $[\mathrm{W\,m^{-2}}]$

q_i Heat flow towards the interior $[\mathrm{W\,m^{-2}}]$

q_e Heat flow towards the exterior $[\mathrm{W\,m^{-2}}]$

θ_d The average temperature of the structure in the axis of the pipes [°C]

θ_e Outside air temperature [°C]

θ_i Inside air temperature [°C]

θ_m Average heating water temperature [°C]

θ_{pi} Interior surface temperature [°C]

θ_{pe} Exterior surface temperature [°C]

Λ_a Thermal permeability of the layer in front of the pipes towards the interior $[\mathrm{W\,(m^2\,K)^{-1}}]$

Λ_b Thermal permeability of the layer behind the pipes towards the exterior $[\mathrm{W\,(m^2\,K)^{-1}}]$

Λ_d Thermal conductivity of the pipe material $[\mathrm{W\,(m^2\,K)^{-1}}]$

λ_a, λ_b Thermal conductivity of the material of the respective layer [W/(m K)]

λ_d Thermal conductivity of the material into which the tubes are inserted [W/(m K)]

References

[1] D. Kalús, P. Páleš, Ľ. Pelachová. Samonosný tepelnoizolačný panel pre systémy s aktívnym riadením prechodu tepla. [Self-supporting thermal insulation panel for systems with active heat transfer control.] (Utility model No. SK 5729 Y1). Úrad priemyselného vlastníctva Slovenskej republiky, 2011. [2022-08-13], https://wbr.indprop.gov.sk/WebRegistre/UzitkovyVzor/Detail/5030-2010.

[2] D. Kalús, P. Páleš, Ľ. Pelachová. Tepelnoizolačný panel pre systémy s aktívnym riadením prechodu tepla. [Thermal insulation panel for systems with active heat transfer control.] (Utility model No. SK 5725 Y1). Úrad priemyselného vlastníctva Slovenskej republiky, 2011. [2022-08-13], https://wbr.indprop.gov.sk/WebRegistre/UzitkovyVzor/Detail/5031-2010.

[3] D. Kalús, P. Páleš, Ľ. Pelachová. Heat insulating panel with active regulation of heat transition (Patent No. EP 2 572 057 B1). European Patent Office, 2011. [2022-08-05], https://patents.google.com/patent/WO2011146025A1/und.

[4] SUNOMAXCUBE. [2022-08-13], https://sunomaxcube.com/.

[5] REHAU. [2022-08-13], https://www.rehau.com/sk-sk.

[6] SUNOMAXCUBE. Individuality in series. [2022-08-13], https://sunomaxcube.com/files/sunomaxcube/sunomaxcube-en.pdf.

[7] Isomax-Terrasol. [2022-08-13], http://www.isomax-terrasol.eu/home.html.

[8] Rieder. [2022-08-13], https://www.rieder.cc/us/.

[9] P. Michalak. Selected aspects of indoor climate in a passive office building with a thermally activated building system: A case study from Poland. *Energies* **14**(4):860, 2021. https://doi.org/10.3390/en14040860.

[10] C. Zhang, M. Pomianowski, P. K. Heiselberg, T. Yu. A review of integrated radiant heating/cooling with ventilation systems- Thermal comfort and indoor air quality. *Energy and Buildings* **223**:110094, 2020. https://doi.org/10.1016/j.enbuild.2020.110094.

[11] X. Wu, L. Fang, B. W. Olesen, et al. Comparison of indoor air distribution and thermal environment for different combinations of radiant heating systems with mechanical ventilation systems. *Building Services Engineering Research and Technology* **39**(1):81–97, 2018. https://doi.org/10.1177/0143624417710105.

[12] M. Krajčík, O. Šikula. The possibilities and limitations of using radiant wall cooling in new and retrofitted existing buildings. *Applied Thermal Engineering* **164**:114490, 2020. https://doi.org/10.1016/j.applthermaleng.2019.114490.

[13] B. Lehmann, V. Dorer, M. Koschenz. Application range of thermally activated building systems tabs. *Energy and Buildings* **39**(5):593–598, 2007. https://doi.org/10.1016/j.enbuild.2006.09.009.

[14] M. Krajčík, M. Arıcı, O. Šikula, M. Šimko. Review of water-based wall systems: Heating, cooling, and thermal barriers. *Energy and Buildings* **253**:111476, 2021. https://doi.org/10.1016/j.enbuild.2021.111476.

[15] M. Schmelas, T. Feldmann, P. Wellnitz, E. Bollin. Adaptive predictive control of thermo-active building systems (TABS) based on a multiple regression algorithm: first practical test. *Energy and Buildings* **129**:367–377, 2016. https://doi.org/10.1016/j.enbuild.2016.08.013.

[16] K.-N. Rhee, K. W. Kim. A 50 year review of basic and applied research in radiant heating and cooling systems for the built environment. *Building and Environment* **91**:166–190, 2015. Fifty Year Anniversary for Building and Environment, https://doi.org/10.1016/j.buildenv.2015.03.040.

[17] J. Xie, X. Xu, A. Li, Q. Zhu. Experimental validation of frequency-domain finite-difference model of active pipe-embedded building envelope in time domain by using Fourier series analysis. *Energy and Buildings* **99**:177–188, 2015. https://doi.org/10.1016/j.enbuild.2015.04.043.

[18] F. Niu, Y. Yu. Location and optimization analysis of capillary tube network embedded in active tuning building wall. *Energy* **97**:36–45, 2016. https://doi.org/10.1016/j.energy.2015.12.094.

[19] M. Krzaczek, J. Florczuk, J. Tejchman. Improved energy management technique in pipe-embedded wall heating/cooling system in residential buildings. *Applied Energy* **254**:113711, 2019. https://doi.org/10.1016/j.apenergy.2019.113711.

[20] T. Kisilewicz, M. Fedorczak-Cisak, T. Barkanyi. Active thermal insulation as an element limiting heat loss through external walls. *Energy and Buildings* **205**:109541, 2019. https://doi.org/10.1016/j.enbuild.2019.109541.

[21] R. Karadağ. New approach relevant to total heat transfer coefficient including the effect of radiation and convection at the ceiling in a cooled ceiling room. *Applied Thermal Engineering* **29**(8):1561–1565, 2009. https://doi.org/10.1016/j.applthermaleng.2008.07.005.

[22] M. Krzaczek, Z. Kowalczuk. Thermal barrier as a technique of indirect heating and cooling for residential buildings. *Energy and Buildings* **43**(4):823–837, 2011. https://doi.org/10.1016/j.enbuild.2010.12.002.

[23] C. Shen, X. Li. Energy saving potential of pipe-embedded building envelope utilizing low-temperature hot water in the heating season. *Energy and Buildings* **138**:318–331, 2017. https://doi.org/10.1016/j.enbuild.2016.12.064.

[24] B. V. Stojanović, J. N. Janevski, P. B. Mitković, et al. Thermally activated building systems in context of increasing building energy efficiency. *Thermal science* **18**(3):1011–1018, 2014. https://doi.org/10.2298/TSCI1403011S.

[25] Y. Yu, F. Niu, H.-A. Guo, D. Woradechjumroen. A thermo-activated wall for load reduction and supplementary cooling with free to low-cost thermal water. *Energy* **99**:250–265, 2016. https://doi.org/10.1016/j.energy.2016.01.051.

[26] J. Babiak, B. W. Olesen, D. Petras. Low temperature heating and high temperature cooling. Embedded water based surface heating and cooling systems. Finnish Association of HVAC Societies FINVAC, 2009. [2022-08-05], https://www.osti.gov/etdeweb/biblio/1030138.

[27] D. Petráš. *Nízkoteplotní vytápění a obnovitelné zdroje energie. Bratislava.* JAGA group, 2008. ISBN 978-80-8076-069-4.

[28] D. Petráš, D. Kalús, D. Koudelková. *Vykurovacie sústavy, cvičenie a ateliérová tvorba.* STU, Bratislava, 2012. ISBN 978-80-227-3795-1.

[29] P. Janík. *Optimization of energy systems with long-term heat accumulation.* Ph.D. thesis, Slovak University of Technology in Bratislava, Faculty of Civil Engineering, 2013. SvF-13422-16657.

[30] European Committee for Standardization. Heating systems in buildings - Design of embedded water based surface heating and cooling systems - Part 1: Determination of the design heating and cooling capacity (Standard No. EN 15377-1:2008).

[31] Úrad pre normalizáciu, metrológiu a skúšobníctvo SR. Thermal protection of buildings. Thermal performance of buildings and components. Part 2: Functional requirements (Standard No. STN 73 0540-2+Z1+Z2).

[32] M. Šimko, M. Krajčík, O. Šikula, et al. Insulation panels for active control of heat transfer in walls operated as space heating or as a thermal barrier: Numerical simulations and experiments. *Energy and Buildings* **158**:135–146, 2018. https://doi.org/10.1016/j.enbuild.2017.10.019.

[33] B. Ning, S. Schiavon, F. S. Bauman. A novel classification scheme for design and control of radiant system based on thermal response time. *Energy and Buildings* **137**:38–45, 2017. https://doi.org/10.1016/j.enbuild.2016.12.013.

[34] S. A. Al-Sanea, M. Zedan, S. Al-Hussain. Effect of thermal mass on performance of insulated building walls and the concept of energy savings potential. *Applied Energy* **89**(1):430–442, 2012. https://doi.org/10.1016/j.apenergy.2011.08.009.

[35] M. Schmelas, T. Feldmann, P. Wellnitz, E. Bollin. Adaptive predictive control of thermo-active building systems (TABS) based on a multiple regression algorithm: First practical test. *Energy and Buildings* **129**:367–377, 2016. https://doi.org/10.1016/j.enbuild.2016.08.013.

[36] E. Nemethova, D. Petras, M. Krajcik. Indoor environment in a high-rise building with lightweight envelope and thermally active ceiling. In *CLIMA 2016: Proceedings of the 12th REHVA World Congress*, vol. 22. 2016.

[37] J. Široký, F. Oldewurtel, J. Cigler, S. Prívara. Experimental analysis of model predictive control for an energy efficient building heating system. *Applied Energy* **88**(9):3079–3087, 2011. https://doi.org/10.1016/j.apenergy.2011.03.009.